



On The In-pipe Inspection Robots Traversing Through Elbows

M. M. Moghaddam^{a,*}, S. Jerban^b

^aDepartment of Mechanical Engineering, Faculty of Engineering, Tarbiat Modares University, Tehran, Iran

^bDépartement de Génie Mécanique, Université de Sherbrooke, Sherbrooke, QC Canada J1K 2R1

ARTICLE INFO

Article history:

Received: May 20, 2015.

Received in revised form:
September 02, 2015.

Accepted: August 24, 2015.

Keywords:

in-pipe robot
inspection robot
elbow
adjustable diameter

ABSTRACT

A general robotic mechanism was presented for in-pipe inspection of level pipes with varied diameter or curved pipelines. The robot employed three legs comprised of parallelogram linkages mechanism which enables adapting to various elbow joints in the piping systems. The curvatures in pipeline are the most important constraints in front of the robot through navigation process. To study the adaptability of in-pipe robots to the elbow, geometrical analysis was used to determine the minimum required diameter of an assumed resizable cylinder when it traverses through elbows. The contact points of the cylinder and the elbow are located at the medial longitudinal cross section of the elbow. However, for any designed configuration of the robots, the contact points are located at other longitudinal cross sections. For any elbow joint, a 3D space, so-called “curved pipe limited area” was defined using the minimum required width along all longitudinal cross sections in elbows. The traversing robot should be adaptable to this limited area which is a function of robot’s length, pipes’ diameter and radius of curvature. A set of computer simulation was used to verify the derived analytical equations. The verified equations in this paper enable designers to confirm the dimensions of the robots for guaranteed traversing through standard elbows in pipeline. In addition to optimizing the robot’s dimensions in designing process, the proposed equations can be used for active controlling of robot’s diameter when it traverses through elbows.

1. Introduction

Pipelines are widely used in power and chemical plants as well as the gas, oil and water supply systems. The inspection process of such pipelines is an important task. Employing in-pipe robots will increase the efficiency and accuracy of pipe inspection, which in turn will reduce the maintenance time and cost of piping systems.

In-pipe inspection robots have been presented with different motion mechanisms including wheeled [1–16], screw principle [11], [14], inchworm [17–19], snakelike type [20–22] and tracked legs [10], [23] mechanisms.

The wheeled type can be considered as the simplest one with an adjustable speed in pipelines [1–16]. The screw based robots were mainly designed for constant size pipelines [11] and [14]. Such robots utilize tilted wheels rotating about the pipe axis to provide forward motion in a manner of a turning screw [11] and [14]. The inchworm type is made up of several units that work in radial and axial contraction-extraction mode. To move forward, the front unit grips the pipe wall and pulls the rear unit then consequently the rear unit grips the pipe wall and pushes the front unit [17–19]. The inchworm type provides a high level of accuracy in positioning but

* Corresponding address: Tarbiat Modares University, Jalal Al Ahmad Ave, Tehran, Iran Tel : 82883358 fax: 88005040
E-mail address: m.moghaddam@modares.ac.ir

a low speed motion. The snakelike is a multi-segment mechanism with a low speed motion that derives propulsion from wheels, legs or tracks on each segment and provides steering abilities in curved pipes [20–22]. The tracked legs type involves a set of tracked units to move forward with a proper speed in pipes [10] and [23]. This mechanism also enables passing small obstacles such as harsh welding joints [10] and [23].

Most of the reported in-pipe robots were designed to be adaptable to small changes of pipe diameter. To hold the wall pipe and move forward in an inclined or a vertical pipe, the robot should provide the necessary friction force. For that purpose, a pre-force should be applied on the wall by the driving wheels or tracks. Many in-pipe robots utilized elastic parts (i.e. spring) [2], [4] and [5] or a linear actuator [1] and [16] or both of them [23] to press the wheels or tracks against the pipe wall. The elastic object provides the required flexibility and presses the wheels against the wall in a passive approach and the pre-force will change for different pipe size due to different spring compression [2], [4] and [5]. However, utilizing the linear actuator does not produce flexibility but an adjustable pre-force on the pipe wall is expected [16].

Usually in pipelines one can expect level pipes, vertical pipes, elbows, branches, reducers and valves. These induce geometric constraints and the robot should be designed such that it can overcome and traverse through successfully. The curvature of the pipelines is the main constraint and the robot should adapt itself by reducing its diameter to pass through them. The problem of the adaptability of the in-pipe robots traversing through elbows or curved pipes is an important issue to be considered in designing and controlling of such robots.

In this paper, we present a generic design of robots for in-pipe inspection which can provide proper pre-force in vertical pipes. We also present how the main dimensions of an in-pipe robot can be designed to be able to pass through all standard elbows in pipeline. The robot employs three legs which are spaced out circumferentially and symmetrically. Each leg has a set of parallelogram linkages to adjust the robot radially inside the pipe and also to traverse through pipelines with variable diameter as well as elbows. So far, this configuration (three symmetric legs) has been used widely for in-pipe inspection robots [1], [16] and [23].

The robot's adaptability has been studied when it traverses through an elbow. Accordingly, the minimum required diameter for the robot with a specific length has been calculated. Firstly, the designer should estimate the probable length of robot according to the size of robot's components. Then in the light of the proposed equations in this paper the minimum required diameter of the robot

can be calculated. Regarding the geometrical restrictions induced by an elbow, the calculated minimum required diameter is less than the targeted pipe size.

Besides, when the robot traverses through elbows, its controller should reduce the diameter by following the proposed equations in this paper to have an appropriate controlling system.

2. Mechanism description

In-pipe inspection robots generally employ three sets of symmetrical leg to adjust the diameter of the robot in pipelines. As an example, four prototyped in-pipe robots with three legs are shown in Figure 1, where the legs are circumferentially spaced out 120° apart to keep the robot in center of the pipeline.

In Figures 1(a), (b) and (c), to adjust the diameter of the robot, a central threaded nut connected to the legs, moves backward or forward by turning a screw. The central screw is driven by an actuator and the tractive force in pipeline can be regulated. Optimizing the pitch of the central screw should conclude a self-locked screw to avoid damaging the actuator in the case of an external impact. In Figure 1(d), a slider connected to the rear legs slides on unthreaded central axis and a linear spring forces the robot to adapt its diameter to the pipeline passively. Employing the linear spring provides the robot an adequate flexibility to pass over obstacles but the pre-force can't be regulated.

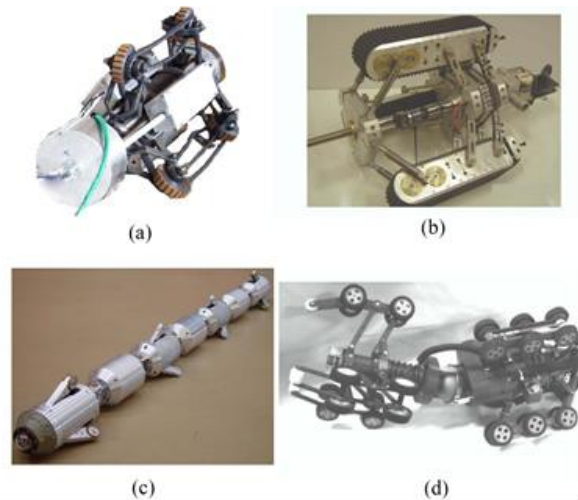


Figure 1: Four prototyped in-pipe robots with three symmetrical legs presented by Z. Yunwei et al. (a) [1], M. M Moghaddam et al. (b) [23], H. Schempf et.al. (c) [16], H. R. Choi et. al. (d) [2].

To evaluate the results of geometrical analysis with a simulated in-pipe robot traversing through elbows a robot with three symmetric legs is designed and modeled. The robot is modeled using Solidworks software and simulated by integrating Visual Nastran with Matlab Simulink software. The modeled robot,

shown in Figure 2, can pass through pipes of 100-200 mm diameter and standard elbows of 150-200 mm diameter (radius of the elbow = 0.75 pipe diameter). When the central slider moves backward, the diameter of the robot will decrease and as it moves forward, the diameter of the robot will increase. To increase the flexibility and adaptability of the normal force acting upon the pipe's wall, a linear spring is also placed on the central hollow axis of the robot, between the slider and a threaded nut. The threaded nut moves along the central screw assembled into the hollow axis. To let the nut move forward and backward three notches on the hollow axis are considered. The central screw is driven by a DC motor to thrust the threaded nut as well as the slider. The pitch of the screw is selected by considering the self-locking principle. As a result of self-locked screw and the linear spring, the actuator doesn't work continuously and it will act if only if the pre-force or the diameter needs to be regulated.

In the simulated model, the driving power is transferred from a central DC motor to the driving wheels in each leg along a special gearbox, a set of simple gears and a timing belt, respectively. The special gear box involves a worm (driver) and three worm gears (driven). The power will be distributed to all the wheels on each leg using an extra timing belt. When the robot passes the elbows, some wheels may rotate with slippage on the wall due to their equal speeds.

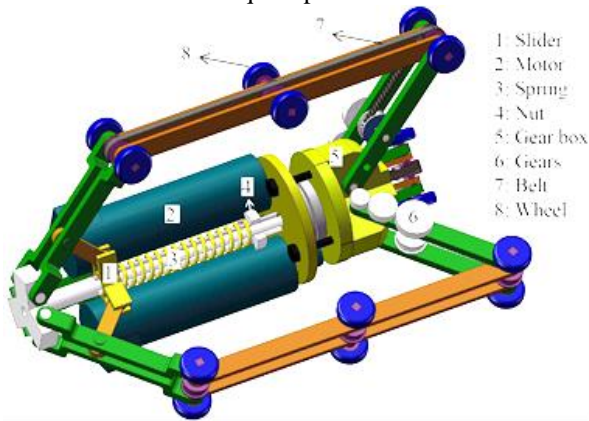


Figure 2: The modeled in-pipe inspection robot and its components

3. Geometrical constraint of an elbow

Few works have been devoted to the adaptability of the in-pipe robots traversing through elbows. Choi et al. [2] have presented a mono segment in-pipe robot in a pipeline that is simply modeled as cylindrical segment. They calculated the maximum length of the cylindrical segment when it is located in a 90° elbow which is a function of diameter of the segment. They used the maximum length and the diameter of the cylindrical segment to estimate if the in-pipe robot can pass through

a 90° elbow or not. They didn't present how the diameter of cylindrical segment (simple model of in-pipe robot) will be adjusted when it is not located completely in elbow. Moreover, the difference between the cylindrical segment and the real configuration of in-pipe robots (a non-cylindrical) where not discussed.

Roh et al. [3] have presented a mono segment in-pipe robot in an elbow that is simplified as two parallel triangles as the set of front and rear wheels [3]. The simplifying triangles are connected using a central line [3]. A set of mathematical equations then are presented to demonstrate the velocity differences for each three wheels due to the motion on the curved path. These equations are used to control the speed of robot traversing through elbow avoiding overloading and slippage in wheels.

Aforementioned methods of simplifying in-pipe robot have some weaknesses. In the cylindrical simplifying [2], the effects of the wheeled legs were not considered. In the second method [3] (two parallel triangles with central line) the effects of the connecting rod between the wheels in parallelogram linkage are not considered.

As illustrated in Figure 3, the width of the pipe section equals $D \cdot \cos \theta$ which varies for different θ that presents the position of the object in pipe section. On the other hand, different θ presents different longitudinal section of the elbow and $\theta = 0$ is representative of medial longitudinal section that has maximum width equal to D . When an object traverses through an elbow, it should reduce its diameter which the reduction magnitude depends on θ .

To study the traversing steps of an object through an elbow with arbitrary angle for different θ , at first we present the equations for the adjusted diameter (maximum diameter) of a traversing object through the elbow when $\theta = 0^\circ$. The object is a $2D$ object with a fixed length yet variable diameter (width). The adjusted diameter of the object for $\theta = 0^\circ$ is equal to the adjusted diameter of a cylindrical segment with the same length. The adjusted width for different θ can be derived later by substituting the pipe's diameter with $D \cdot \cos \theta$.

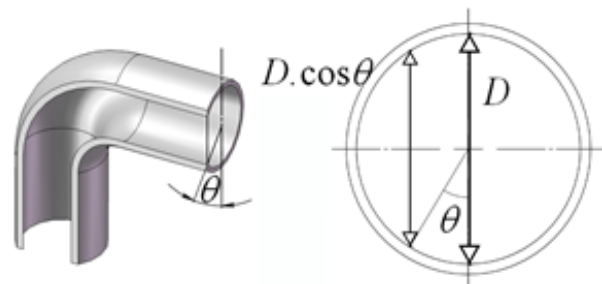


Figure 3: Cross section of the curved pipe

3.1. Traversing a cylinder through elbow

Figure 4 shows the longitudinal cross section of a cylindrical segment in two successive positions in an elbow with an arbitrary curvature angle γ_{curve} . It is assumed that the cylindrical segment has an adjustable diameter, W , yet a fixed length, h . In Figure 4, D and R are the pipe diameter and the radius of the curvature, respectively.

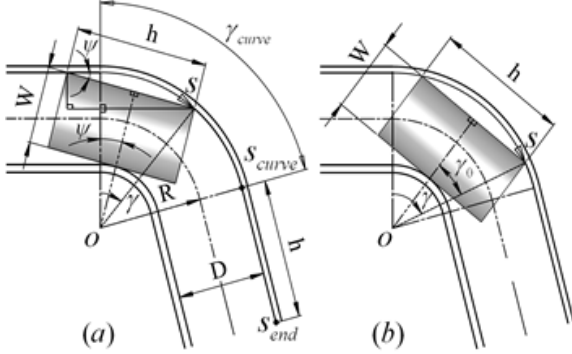


Figure 4: A cylinder traverses through an elbow with an arbitrary angle (a) Entering into the elbow. (b) Completely located in the elbow

As illustrated in Figure 4 (a), the traversed distance is measured for the right-upper-corner of the cylinder as S in respect to the entrance point of the curvature. Accordingly, the traversed angle of the curvature is shown with γ . Eq. (1) shows the relationship between the traversed angle and the traversed distance.

$$s = \gamma \cdot \left(R + \frac{D}{2}\right) \quad (1)$$

When the right-upper-corner of the block reaches to the end of the curved section, the traversed distance s_{curve} is obtained from Eq. (2). However, when the cylinder exits from the curvature completely, the traversed distance equals s_{end} as in Eq. (3).

$$s_{curve} = \gamma_{curve} \cdot \left(R + \frac{D}{2}\right) \quad (2)$$

$$\begin{cases} s_{min} = 0 \\ s_{max} = s_{end} = s_{curve} + h \end{cases} \quad (3)$$

In Figure 4 (b), γ_0 can be defined when a cylinder is completely located in the curved pipe and can be found as:

$$\left(R + \frac{D}{2}\right) \sin \gamma_0 = \frac{h}{2} \Rightarrow \gamma_0 = \text{Arcsin}\left(\frac{h}{2R + D}\right) \quad (4)$$

Figure 4 (a) shows the first stage where the cylindrical segment entered partially into the curvature. Figure 4 (b) shows the second stage where the cylindrical segment is completely in the curvature and $\gamma > 2\gamma_0$. The angle between the side surface of the cylinder and the surface of the entrance level pipe is defined as ψ and it can be derived from geometrical principle as:

$$\psi = \text{Arcsin} \frac{(2R + D)(1 - \cos \gamma)}{2h} \quad (5)$$

Then, the adjusted diameter of the cylinder for the first stage (Figure 4(a)) can be derived as a function of the traversed angle of the curvature as:

$$W = \left(R + \frac{D}{2}\right) \cos(\gamma - \psi) - \left(R - \frac{D}{2}\right) \quad (6)$$

Accordingly, the adjusted diameter of the cylinder for the second stage is:

$$W = \left(R + \frac{D}{2}\right) \cos \gamma_0 - \left(R - \frac{D}{2}\right) \quad (7)$$

As can be seen in Eq. (7), (Figure 4(b)), the adjusted diameter of the cylinder is constant. The second stage (Figure 4(b)) is more critical compared with the first stage (Figure 4(a)) in traversing through the curved pipe, because the required adjusted diameter of the cylinder is less than that of the first stage.

In some cases the cylinder cannot be located in the curvature completely when the curvature angle is relatively small as shown in Figure 5. In such cases, there are two similar stages. The adjusted diameter of the cylinder for the first stage (Figure 5(a)) can be derived from Eq. 6 similarly whereas for the second stage (Figure 5(a)) the story is different. As illustrated in Figure 5(b), in the second stage, two ends of the cylinder are located on the straight parts of the pipeline. The angle between the side surface of the cylinder and the surface of outlet level pipe is defined as ψ' where can be found as:

$$\frac{BC}{\sin \psi'} = \frac{h}{\sin(\pi - \gamma_{curve})} \quad (8)$$

where,

$$BC = s - s_{curve} + \left(R + \frac{D}{2}\right) \cdot \tan\left(\frac{\gamma_{curve}}{2}\right) \quad (9)$$

Accordingly, the adjusted diameter of the cylinder can be found as:

$$W = (R + \frac{D}{2} - (s - s_{curve}) \cdot \tan(\gamma_{curve} - \psi)) \cdot \cos(\gamma_{curve} - \psi) - (R - \frac{D}{2}) \tag{10}$$

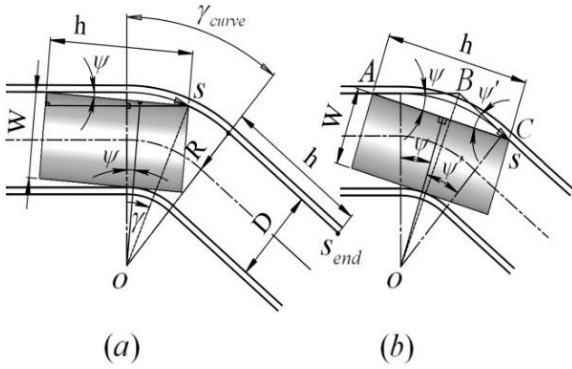


Figure 5: A cylinder traverses through an elbow with an arbitrary angle ($\gamma_{curve} < 2\gamma_0$) when it is (a) entering into the elbow and (b) its two ends are located at the level pipe

Briefly, there are three equations (Eq. 6, Eq. 7 and Eq. 10) to calculate the adjusted diameter of the assumed cylinder traversing through elbows for all stages. The diagram of the adjusted diameter of the cylinder versus the traversed distance is shown in Figure 6 for three types of curvatures; (1) $\gamma_{curve} < 2\gamma_0$, (2) $\gamma_{curve} = 2\gamma_0$ and (3) $\gamma_{curve} > 2\gamma_0$. The minimum cylinder's diameter, D_{min} will be achieved when the traversed angle is equal to $2\gamma_0$ and it can be obtained from Eq. (7) as a function of robot's length, pipe's diameter and radius of the curvature. For example, for the length of our generic modeled robot D_{min} and $2\gamma_0$ will be 129 mm and 57° , respectively. Specifically, the pipe's diameter and radius of the curvature are 152 mm and 114 mm, respectively.

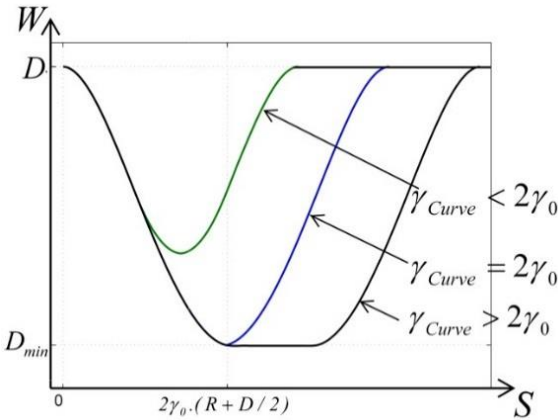


Figure 6: Diagram of the adjusted diameter of the assumed adjustable cylinder through elbow

Right after the cylinder passes the middle of the curvature, the traversing stages will be repeated. In other words; the exiting stages are same as the entering stages. Thus the diagrams are symmetrically allied on the horizontal axis.

3.2. The curved pipe limited area

In section 3.1, we calculated the adjusted diameter of a cylinder with a specific length when it traverses through an elbow. When a cylinder is traversing through an elbow, its contact points with pipe's wall are located at central longitudinal cross section ($\theta = 0^\circ$, Figure 3). But for non-cylindrical objects, the contact points are located at other angles ($\theta \neq 0^\circ$) and the adjusted diameter should be calculated from equations applied to their corresponding longitudinal sections with $\theta \neq 0^\circ$. Indeed, an object with a specific length and any probable configuration can traverse through an elbow when its width can be reduced under the adjusted width W_θ in all longitudinal elbow sections.

As mentioned, denoting the diameter of the pipe with $D \cdot \cos \theta$ (Figure 3) and substituting in Eq. (6), Eq. (7) and Eq. (10), the adjusted width W_θ for different θ can be obtained for all longitudinal sections of the elbow. By utilizing W_θ , we can define a 3D space inside the elbows such that the in-pipe robot should be adapted (inscribable) in it when it traverses the elbow. This assumed 3D space is called as curvature limited area. The front view of the limited area is shown in Figure 7 (a) for the critical stage of the object traversing through the elbow when it is located in the curvature completely. The side view of the curvature limited area is shown in Figure 7(b). In Figure 7(b), the side view ($\theta = 0^\circ$) of the curved pipe's limited area has been illustrated and the dashed line is the trajectory of objects upper contact point in section $C - C'$ when it is traversing through elbow. Figure 7(a) is the front view of the limited area from section $C - C'$ that is object's medial section.

Therefore, if the designer determines the limited area of the elbows based on the robot's length, he or she will be sure that the robot can traverse through elbow or not. The designer can optimize the robot's dimensions via determining the limited areas of the curved pipes. The limited area of the curved pipe has an asymmetric configuration about central point of the pipe section (Figure 7(a)). The cross section of the elbow's limited area is larger than the section of a cylindrical segment (circle) which can cross through the curved pipe.

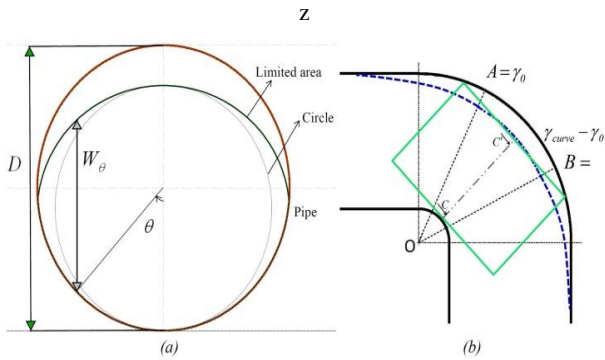


Figure 7: (a) Front view of the limited area of the curved pipe for the most critical stage, when the object is completely located in the curvature (c-c' cross section in (b)). (b) Side view of the limited area of the curved pipe.

In Figure 8, the side view of the limited area and four steps of traversing through elbow are shown when the object is partially in the entrance level pipe (Figure 8 (a)), completely located in the curved pipe (Figure 8 (b)), (c) and partially located in outlet level pipe (Figure 8 (d)). The side view of the elbow's limited area can be assumed as the trajectory of upper point of the medial cross section of the object (referred in Figure 7 (b)).

As can be found from asymmetric configuration of the limited area of the curved pipe, the location angle ζ will determine the required radius of in-pipe robot traversing through the elbow; where, location angle ζ is defined as the direction angle of the robot's leg in respect to the symmetric plane of the elbow ($\theta = 0^\circ$) (Figure 9).

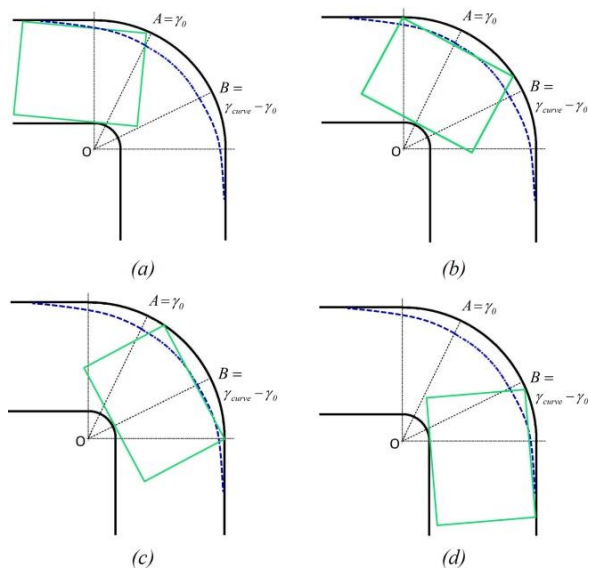


Figure 8: Side view of elbow's limited area at four different steps of traversing through elbow

In Figure 9, the simplified robot cross section is shown

for various location angles from 0° to 60° . The adaptability of in-pipe robot in the limited area of curvature varies, due to the width wheels, b (e.g., in designed robot $b=35 \text{ mm}$). Therefore, the adjusted diameter of in-pipe robot traversing through elbows is a function of location angle; where, the adjusted diameter of the robot is the diameter of a circle which covers the simplified model of the robot's cross section. It should be noted that the center of the robot is not located in the center of the elbow section.

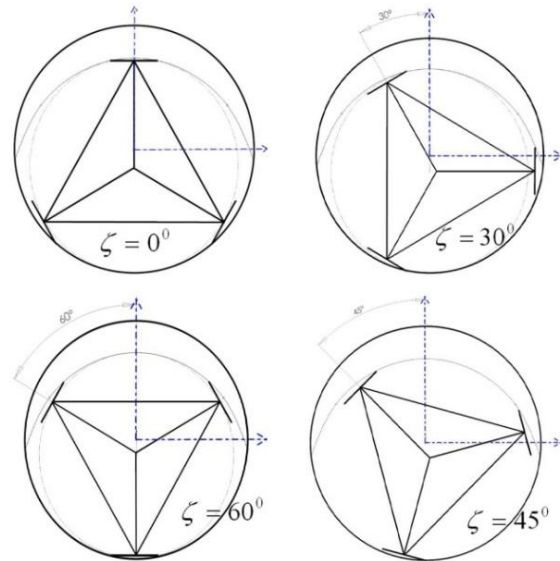


Figure 9: The section of adapted robot inscribed with the limited area of the curved pipe for $\zeta=0^\circ, 30^\circ, 45^\circ$ and 60° .

To show the difference in adaptability for various location angles, the traversing through elbows has been simulated in Visual Nastran software for the modeled in-pipe robot (Figure 2).

The adjusted diameter of the robot is shown for various location angles in Figures 10 and 11 for two different modeled elbows. As illustrated in Figure 10 when the diameter of pipeline is equal to 190 mm , the adjusted diameter of the cylindrical segment from the analytical equations (Figure 6) is less than the adjusted diameter of the in-pipe robot from simulation results. Thus, for any location angle, the in-pipe robot traverses through the elbow easier than the cylindrical segment.

As illustrated in Figure 11, for another instance, when the diameter of pipeline is equal to 150 mm , the width of the wheels (in the modeled is equal to 35 mm) is unneglectable. Therefore, the adjusted diameter of the cylindrical segment from the analytical equations isn't less than the adjusted diameter of in-pipe robot from simulation results.

It should be noted that due the impact principle in simulated contacts (between pipe and robot's wheels)

and the linear spring in the designed model, the simulation diagrams are slightly fluctuating (Figures 11 and 12).

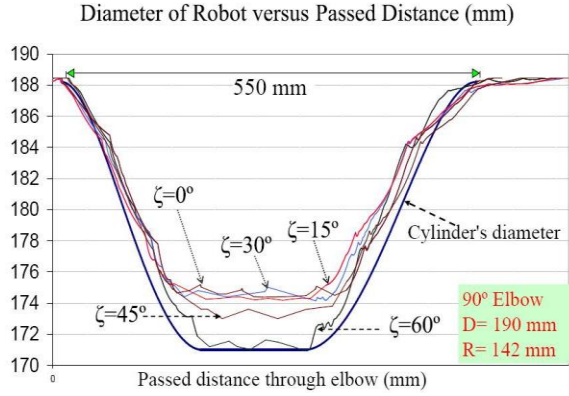


Figure 10: The diameter of the robot vs. the passed distance through 90° elbow with $D=190$, $R=142$ mm

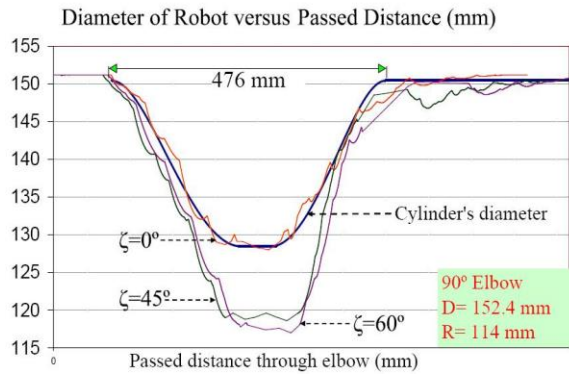


Figure 11: The diameter of the robot vs. the passed distance through 90° elbow with $D=152.4$, $R=114$ mm

Accumulating the above discussion, the width of pair of the wheels in the robot is an important parameter. For wheels with small width, the minimum adjusted diameter of the robot is more than that of a cylindrical segment with same length. Therefore, the optimized dimensions calculated on basis of cylindrical segment traversing through the elbows, in designing process are sufficient, yet for wide wheels (pair wheels) or tracks (Figure 1(b) and Figure 1(d)), the computer simulations of traversing through the elbows is strongly required.

4. Verification the results for $\zeta = 0^\circ$

To verify and demonstrate the presented analytical equations in this paper for describing the limited area of the curved pipe, the required radius of the modeled robot

for $\zeta = 0^\circ$ traversing through the elbows is compared with the analytical equations. Figure 12 shows the simplified model of the in-pipe robot inscribed in the limited area of the elbow. Here, the size of the simplifying triangle of in-pipe robot is indicated by a , therefore the radius of the robot (distance between the middle point of the pair of wheels and the center of the triangle) can be found from Eq. (11). The width of the limited area W_{ob} for $x = b/2$ and can be found by substituting the θ_b (Eq. (12)) in W equations (Eqs. (6), (7) and (10)).

$$R_{Robot} = \frac{a}{\sqrt{3}} \quad (11)$$

$$\theta_b = \text{Arc sin}\left(\frac{b}{D}\right) \quad (12)$$

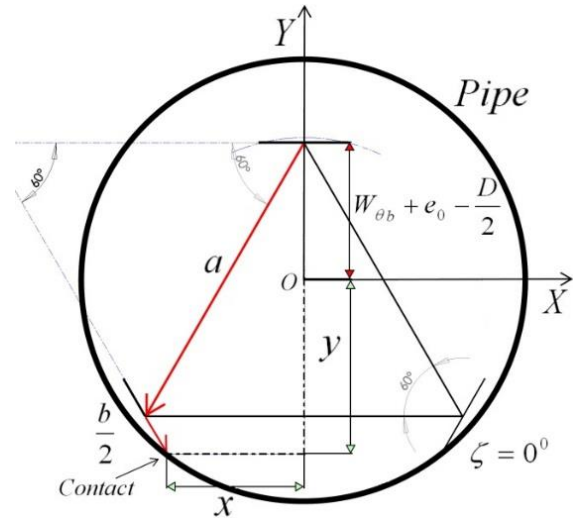


Figure 12: The simplifying triangle model of the robot inscribed in the cross sections of the elbow's limited area for $\zeta = 0^\circ$

The lower contact point (x, y) in Figure 12 locates on the internal surface of the pipe which is a circle. The coordinates of this contact point (x, y) in respect to the pipe's center point can be found as the result of the following vector summation; $\vec{a} + \vec{b}/2$ (Eq. (13)).

$$\begin{cases} I) & x^2 + y^2 = \frac{D^2}{4} \\ II) & x = -a \cdot \cos\left(\frac{\pi}{3}\right) + \frac{b}{2} \cdot \cos\left(\frac{\pi}{3}\right) \\ III) & y = W_{ob} + e_0 - \frac{D}{2} - a \cdot \sin\left(\frac{\pi}{3}\right) - \frac{b}{2} \cdot \sin\left(\frac{\pi}{3}\right) \end{cases} \quad (13)$$

By substituting the Eq. (13-II) and Eq. (13-III) in Eq. (13-I), we can find a second order equation which its regular configuration is written in Eq. (14).

$$Aa^2 + Ba + C = 0$$

$$\begin{cases} A = 1 \\ B = -\sqrt{3}(W_{\theta b} + e_0 - \frac{D}{2} - \frac{(\sqrt{3}-1)b}{4}) \\ C = (W_{\theta b} + e_0 - \frac{D}{2} - \frac{\sqrt{3}b}{4})^2 + \frac{b^2}{16} - \frac{D^2}{4} \end{cases} \quad (14)$$

In Figure 13, 14 and 15, the calculated radius of the in-pipe robot from simulations are compared with analytical results (Eqs. (11) and (14)) for $\zeta = 0^0$ in three different elbows. Specifically, the calculated radiuses versus the passed distance of 60°, 75° and 90° elbows in 150 mm pipeline are shown in Figures 13, 14 and 15, respectively. The analytical results are very consistent with the simulation results. These comparisons confirm the accuracy in both analytical and the simulation results presented in this article.

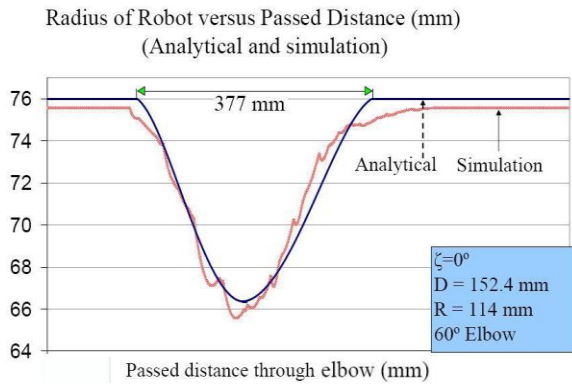


Figure 13: Calculated radius of the robot vs. the passed distance of elbow from analytical and simulation methods. The elbow angle equals 60° ($\zeta = 0^0$, D=152.4, R=114 mm)

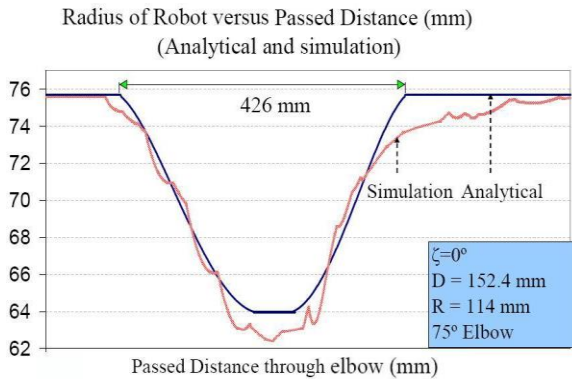


Figure 14: Calculated radius of the robot vs. the passed distance of elbow from analytical and simulation methods. The elbow angle equals 75° ($\zeta = 0^0$, D=152.4, R=114 mm)

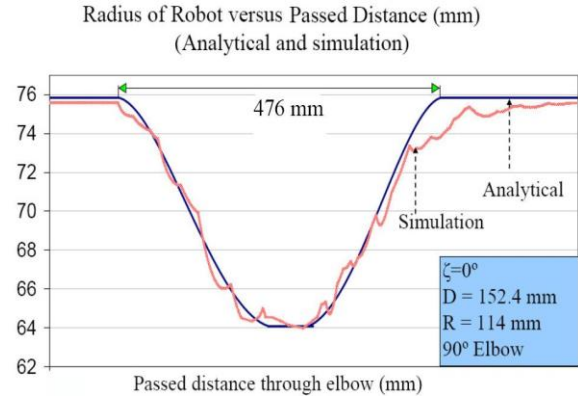


Figure 15: Calculated radius of the robot vs. the passed distance of elbow from analytical and simulation methods. The elbow angle equals 90° ($\zeta = 0^0$, D=152.4, R=114 mm).

5. Conclusion

The diameter of in-pipe robot should be adjusted when it traverses through elbows. Using the geometrical/analytical equations, the minimum required diameter of a resizable cylinder traversing through a curved pipe is calculated, which is a function of the pipeline diameter, curvature radius, curvature angle and length of the robot.

The resizable cylinder has only two contact points located at medial longitudinal cross section of the elbow ($\theta = 0^0$). However, the contact points of the generic in-pipe robot may locate in any other longitudinal sections. Therefore the adjusted diameter is then calculated for all longitudinal cross sections ($\theta \neq 0^0$) to define the limited area of the elbow. The elbow's limited area is a 3D space that the robot should be adapted in, when it is traversing through the elbow.

Based on the proposed equations for the curved pipe's limited area in this paper, the designer will be sure that the robot with a specific length can pass through a standard elbow or not. For the robots with narrow wheels, the designer can use directly the Eqs. (6), (7) and (10); but, the simulation results of traversing through the elbows are required for relatively wide wheels or tracks (Figure 1(b) and 1(d)). For wide wheels or tracks, using the presented equations multiplied by a safety factor can be useful.

As a result of asymmetric configuration of the limited area of the curved pipe, the location angle described in this article, ζ , also plays an essential role, particularly in the case of wide wheels. Comparing the results of simulations with the analytical method for $\zeta = 0^0$ confirms the accuracy of the derived equations of adjusted diameter for traversing robot through elbow.

6. References

- [1] Y. Zhang, G. Yan, In-pipe inspection robot with active pipe-diameter adaptability and automatic tractive force adjusting, *Mech. Mach. Theory*, Vol. 42(12), (2007), 1618–1631.
- [2] H. R. Choi, S. M. Ryew, Robotic system with active steering capability for internal inspection of urban gas pipelines, *Mechatronics*, Vol. 12(5), (2002), 713–736.
- [3] S. G. Roh, H. R. Choi, Differential-drive in-pipe robot for moving inside urban gas pipelines, *IEEE Trans. Robotics*, Vol. 21(1), (2005), 1–17.
- [4] S. Hirose, H. Ohno, T. Mitsui, and K. Suyama, Design of In-pipe Inspection Vehicles for $\phi 25$, $\phi 50$, $\phi 150$ pipes, *IEEE Int. Conf. Robot. Autom.* (May), (1999), 2309–2314.
- [5] K. Suzumori, T. Miyagawa, M. Kimura, and Y. Hasegawa, Micro inspection robot for 1-in pipes, *IEEE/ASME Trans. Mechatronics*, Vol. 4(3), (1999), 286–292.
- [6] H. Qi, X. Zhang, H. Chen, and J. Ye, Tracing and localization system for pipeline robot, *Mechatronics*, Vol. 19(1), (2009), pp. 76–84.
- [7] O. Tătar, D. Măndru, and I. Ardelean, Development of mobile minirobots for in pipe inspection tasks, *Mechanika*, Vol. 68(6), (2007), 60–64.
- [8] C. J. C. Jun, Z. D. Z. Deng, and S. J. S. Jiang, Study of Locomotion Control Characteristics for Six Wheels Driven In-Pipe Robot, 2004 *IEEE Int. Conf. Robot. Biomimetics*, (2004), 119–124.
- [9] S. Roh, H. Choi, Strategy for navigation inside pipelines with differential-drive inpipe robot, *Proc. 2002 IEEE Int. Conf. Robot. Autom.* (Cat. No.02CH37292), Vol. 3(May), (2002), 2575–2580.
- [10] N. S. Roslin, A. Anuar, M. F. A. Jalal, and K. S. M. Sahari, A Review: Hybrid Locomotion of In-pipe Inspection Robot, *Procedia Eng.*, Vol. 41, (2012), 1456–1462.
- [11] L. Qingyou, R. Tao and Y. Chen, Characteristic analysis of a novel in-pipe driving robot, *Mechatronics*, Vol. 23(4), (2013), 419–428.
- [12] D. Lee, J. Park, D. Hyun, G. Yook, and H. S. Yang, Novel mechanisms and simple locomotion strategies for an in-pipe robot that can inspect various pipe types, *Mech. Mach. Theory*, Vol. 56,(2012), 52–68.
- [13] M. R. A. M. Zin, K. S. M. Sahari, J. M. Saad, A. Anuar, and A. T. Zulkarnain, Development of a Low Cost Small Sized In-Pipe Robot, *Procedia Eng.*, Vol. 41, (2012), 1469–1475.
- [14] A. Nayak and S. K. Pradhan, Design of a New In-Pipe Inspection Robot, *Procedia Eng.*, Vol. 97, (2014), 2081–2091.
- [15] K. U. Scholl, V. Kepplin, K. Berns, and R. Dillmann, An articulated service robot for autonomous sewer inspection tasks, *Proc. 1999 IEEE/RSJ Int. Conf. Intell. Robot. Syst. Hum. Environ. Friendly Robot. with High Intell. Emot. Quotients* (Cat. No.99CH36289), Vol. 2, (1999), 1075–1080.
- [16] H. Schempf, E. Mutschler, V. Goltsberg, G. Skoptsov, A. Gavaert, and G. Vradis, Explorer: Untethered Real-time Gas Main Assessment Robot System, *System*, (2003).
- [17] J. Lim, H. Park, J. An, Y. S. Hong, B. Kim, and B. J. Yi, One pneumatic line based inchworm-like micro robot for half-inch pipe inspection, *Mechatronics*, Vol. 18(7), (2008), 315–322.
- [18] J. Qiao, J. Shang, and A. Goldenberg, Development of inchworm in-pipe robot based on self-locking mechanism, *IEEE/ASME Trans. Mechatronics*, Vol. 18(2) ,(2013), 799–806.
- [19] C. Anthierens, a. Ciftci, and M. Betemps, Design of an electro pneumatic micro robot for in-pipe inspection, *ISIE '99. Proc. IEEE Int. Symp. Ind. Electron.* (Cat. No.99TH8465), Vol. 2(3), (1999), 968–972.
- [20] M. Hara and S. Satomura, Control of a snake-like robot using the screw drive mechanism, *Robot*, April, (2007), 10–14.
- [21] S. Wakimoto, J. Nakajima, M. Takata, T. Kanda, and K. Suzumori, A micro snake-like robot for small pipe inspection, *MHS2003. Proc. 2003 Int. Symp. Micromechatronics Hum. Sci.* (IEEE Cat. No.03TH8717), (2003), 1–6.
- [22] K. Suzumori, S. Wakimoto, and M. Takata, A miniature inspection robot negotiating pipes of widely varying diameter, 2003 *IEEE Int. Conf. Robot. Autom.* (Cat. No.03CH37422), Vol. 2, (2003), 2735–2740.
- [23] M. M. Moghaddam and M. R. a. Tafti, Design, modeling and prototyping of a pipe inspection robot, *Int. Symp. Autom. Robot. Constr.*, (2005), 1–6.

Biography



Majid M. Moghaddam received the PhD in mechanical engineering from the University of Toronto, Canada, in 1996. He is a professor of mechanical engineering at Tarbiat Modares University, Tehran, Iran. His current research, which focuses on applied robotics and robust control, is concerned with haptic robotics, rehabilitation robotics, inspection robotics, and rough terrain mobile robot design. He is a member of the Administrative Committee of Robotics and Mechatronics Societies of Iran.



Saeed Jerban has received his B.Sc. and M.Sc. degrees in Mechanical Engineering from University of Mazandaran (Babol, Iran) and Tarbiat Modares University (Tehran, Iran), respectively. Since summer 2011, Saeed is a PhD student at the Mechanical Engineering department in Université de Sherbrooke, Québec, Canada.